Bone Tumors and Tumorlike Conditions: Analysis with Conventional Radiography[1]

Theodore T. Miller, MD

The approach to the radiographic diagnosis of bone tumors consists of analyzing the lesion in an organized fashion, with attention to the specific radiographic features of tumor location, margins, and zone of transition; periosteal reaction; mineralization; size and number of lesions; and presence of a soft-tissue component. Patient age is also an important clinical factor in the diagnosis of bone tumors, because various lesions have predilections for specific age groups.

[1] From the Department of Radiology and Imaging, Hospital for Special Surgery, 535 E 70th St, New York, NY 10021. Received June 15, 2006; revision requested August 7; revision received December 9, 2007; accepted February 9; final version accepted April 9; final review and update by the author, October 3. **Address correspondence to** the author (e-mail: *millertt@hss.edu*).

The term *bone tumor* is a broad category, encompassing benign and malignant neoplasms, reactive focal abnormalities, metabolic abnormalities, and miscellaneous "tumorlike" conditions. This article will categorize bone tumors according to their classic appearances and typical patient age groups, but radiographic exceptions always exist and ages should be considered approximate. In addition, this article is not going to discuss any particular tumor in depth; the interested reader should further his or her knowledge by reading any standard textbook chapter or review article on specific tumors. The purpose of the tables in this article is merely to help the reader organize his or her understanding of these abnormalities rather than to provide lists for memorization; it is better to recognize the predilection of different lesions for certain locations and age groups and to understand how to analyze the radiographic appearances of these lesions than it is to memorize long lists.

Table 1

Peak Age Predilection of Bone Lesions

Age (y)	Benign	Malignant
<20	Fibrous cortical defect, nonossifying fibroma, simple bone cyst, aneurysmal bone cyst, chondroblastoma, Langerhans cell histiocytosis, osteoblastoma, osteoid osteoma, osteofibrous dysplasia, chondromyxoid fibroma, fibrous dysplasia, enchondroma	Leukemia, Ewing sarcoma, osteosarcoma (conventional, periosteal, telangiectatic), metastatic disease (rare), neuroblastoma, retinoblastoma, rhabdomyosarcoma, Hodgkin lymphoma
20–40	Enchondroma, giant cell tumor, osteoblastoma, osteoid osteoma, chondromyxoid fibroma, fibrous dysplasia	Osteosarcoma (parosteal), adamantinoma
>40	Fibrous dysplasia, Paget disease, non-Hodgkin lymphoma, chondrosarcoma, malignant fibrous histiocytoma, osteosarcoma (secondary to Paget disease and radiation)	Metastatic disease (most common), myeloma

Figure 1

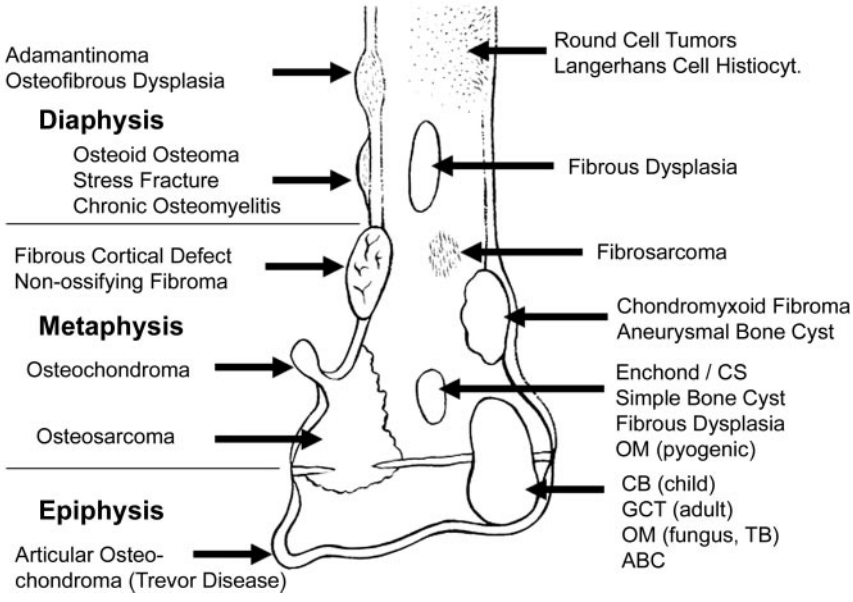

Figure 1: Diagram shows common locations of tumors and tumorlike conditions in transverse and longitudinal dimensions of a long bone. *ABC* = aneurysmal bone cyst, *CB* = chondroblastoma, *CS* = chondrosarcoma, *Enchond* = enchondroma, *GCT* = giant cell tumor, *OM* = osteomyelitis, *TB* = tuberculosis. (Adapted and reprinted, with permission, from reference 1.)

Essentials

- Tumors have a typical patient age range—<20, 20–40, and >40 years old—and a typical location in the skeleton—flat versus tubular bones, epiphyseal versus metaphyseal versus diaphyseal, or medullary versus cortical versus juxtacortical.
- The margin of a lesion and type of periosteal reaction are indicators of lesion aggressiveness, but not necessarily of whether it is benign or malignant: A well-defined lesion with a sclerotic rim and thick unilamellar periosteal reaction is the most innocuous appearance, while a permeated pattern with spiculated periosteal reaction is the most aggressive.
- The pattern of mineralization of the tumor matrix is often the clue to the type of tumor: Mineralization of chondral tissue is punctate, flocculent, or arclike, while mineralization of osseous tissue is fluffy and cloudlike.

Approach

The two most important aspects of evaluating a bone tumor are the location of

Published online before print
10.1148/radiol.2463061038

Radiology 2008; 246:662–674

Author stated no financial relationship to disclose.

the tumor and the age of the patient. Knowledge of this information alone is enough to narrow the differential diagnosis without even looking at any images. The specific radiographic appearance should then help narrow the list even further and will often lead to the single correct diagnosis.

The approach to the radiographic diagnosis of bone tumors consists of analyzing the lesion in an organized fashion, with attention paid to several specific radiographic features (1–5). While these features were originally described with reference to the appearance of the lesion on conventional radiographs, they can also be applied to computed tomographic (CT) images (6). However, they cannot be applied to magnetic resonance (MR) images, because the aggressiveness of some benign lesions can be overestimated on MR images as a result of marrow and soft-tissue edema (7–9). The specific radiographic features that should be evaluated are tumor location, margins and zone of transition, periosteal reaction, mineralization, size and number of lesions, and presence of a soft-tissue component.

Patient Age

Most bone tumors have a predilection for a specific age group; therefore, the most important piece of clinical information when assessing a bone tumor is the patient's age. Exceptions do exist, but the

Table 2

Typical Locations of Bone Lesions

Location	Benign	Malignant
Epiphyseal (end of bone)	Chondroblastoma (skeletally immature patient)	Clear cell chondrosarcoma (exceedingly rare tumor)
	Giant cell tumor (skeletally mature patient)	
	Osteomyelitis (pyogenic: starts in metaphysis and may spread to epiphysis if the person is <18 mo old; tuberculosis or fungus at end of bone in skeletally mature person)	
	Paget disease	
	Intraosseous ganglion/geode (should have associated arthritis)	
	Osteochondral injury	
Metaphyseal		
Medullary	Simple (unicameral) bone cyst (centrally located)	Conventional osteosarcoma
	Aneurysmal (multicameral) bone cyst (eccentrically located; may be engrafted on other lesions such as giant cell tumor and chondroblastoma)	Chondrosarcoma
	Enchondroma (centrally located)	Metastatic disease
	Fibrous dysplasia	Myeloma (over age 40)
	Osteomyelitis (typical location for pyogenic infection in children >18 mo and adults)	Lymphoma
	Localized Langerhans cell histiocytosis	Malignant vascular tumors (very rare; angiosarcoma, hemangiopericytoma)
	Chondromyxoid fibroma (eccentrically located)	
Cortical	Fibrous cortical defect and nonossifying fibroma (lytic in children, fills in and involutes in adults)	Metastatic disease (especially lung)
	Osteoid osteoma (small lucent nidus with surrounding fusiform reactive sclerosis)	
Juxtacortical	Juxtacortical chondroma (arises from periosteum)	Periosteal osteosarcoma (arises from deep cambian layer of periosteum)
		Parosteal osteosarcoma (arises from a superficial layer of periosteum)
		Juxtacortical chondrosarcoma (arises from the periosteum)
Diaphyseal (shaft)		
Medullary	Fibrous dysplasia	Ewing sarcoma (may also occur in the metaphysis and in flat bones: eg, calvarium, pelvis, mandible, ribs; reflecting red marrow distribution)
	Localized Langerhans cell histiocytosis (may also occur in metaphysis and flat bones, eg, calvarium, pelvis, mandible, ribs)	Lymphoma
		Myeloma (occurs in red marrow sites, eg, axial skeleton and proximal aspects of humeri and femora)
		Metastatic disease (may be medullary or cortical)
		Malignant vascular tumors (very rare; angiosarcoma, hemangiopericytoma)
Cortical	Ossifying fibroma (ie, osteofibrous dysplasia or Campanacci lesion)	Adamantinoma (mixed lytic and sclerotic lesion occurring almost exclusively in anterior cortex of tibia; tibia may be bowed; look for satellite lesion in tibia or adjacent fibular involvement)
		Metastatic disease (especially lung)

typical peak ages of different lesions are listed in Table 1. For example, simple bone cysts and chondroblastomas occur in skeletally immature people, while giant cell tumors occur in skeletally mature people. Ewing sarcoma typically occurs in 10–20-year-old patients, while conventional osteosarcoma has two age peaks, one, arising de novo, in teenagers and the second, arising in pagetic or previously irradiated bone, in adults older than 50 years. A malignant bone lesion in an adult over 40 years old is much more likely to be metastatic carcinoma, myeloma, or metastatic non-Hodgkin lymphoma rather than a primary bone sarcoma.

Location

Most bone tumors, regardless of whether they are benign or malignant, often occur in a characteristic location in the skeleton (ie, axial vs appendicular skeleton or long vs flat bone). Thus, some tumors (eg, osteosarcoma) have a predilection for sites of rapid bone growth, usually the metaphyseal region, while other tumors (eg, Ewing sarcoma) tend to follow the distribution of red marrow. Furthermore, a lesion in a long bone may be characterized by its longitudinal location (epipyseal vs metaphyseal vs diaphyseal) and by its transverse location (medullary vs cortical vs juxtacortical). For example, a simple bone cyst and a nonossifying fibroma are both metaphyseal lesions, but the simple bone cyst is a medullary process, while the nonossifying fibroma is a cortical process. Moreover, a simple bone cyst

Figure 2

Figure 2: Anteroposterior radiograph of the hip in a 17-year-old patient shows lucent, mildly expansile lesion (arrows) in the greater trochanter (an epiphyseal equivalent), representing chondroblastoma.

Figure 3

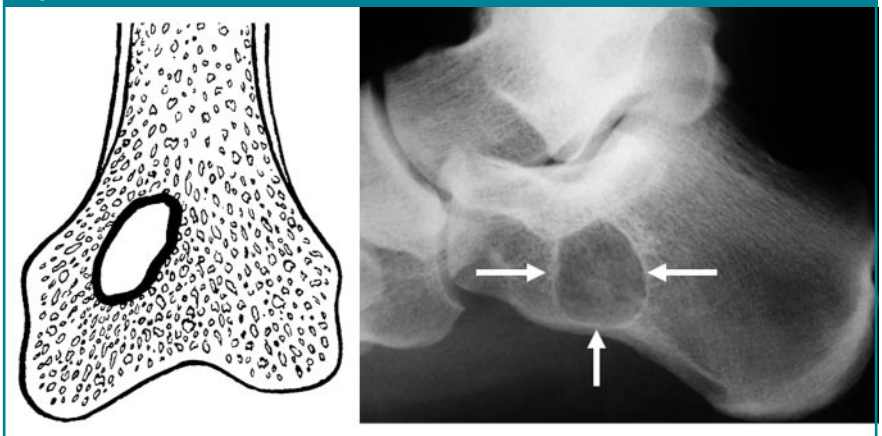

a. b.

Figure 3: Type 1a geographic lesion. **(a)** Diagram shows well-defined lucency with sclerotic rim. (Adapted and reprinted, with permission, from reference 1.) **(b)** Lateral radiograph shows intraosseous lipoma of the calcaneus, with a sclerotic rim (arrows).

Figure 4

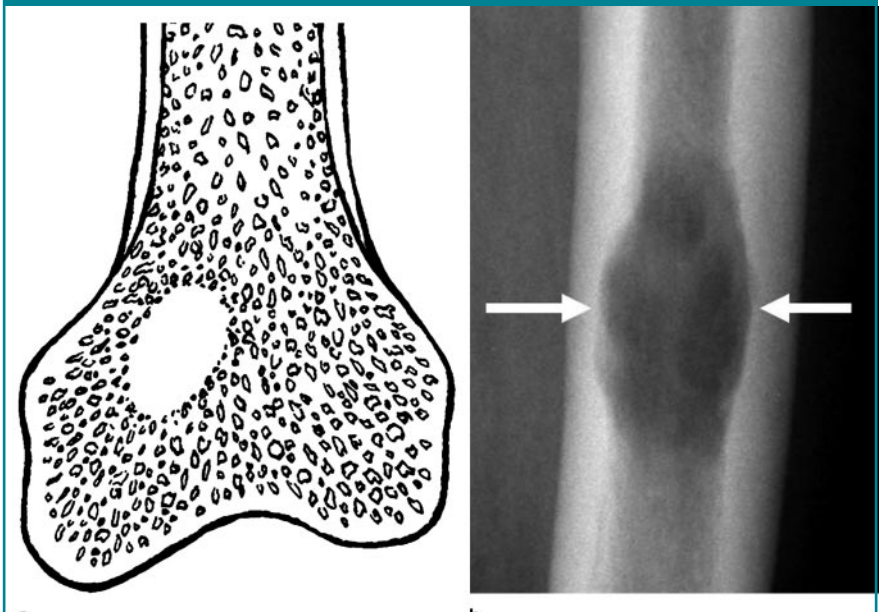

a. b.

Figure 4: Type 1b geographic lesion. **(a)** Diagram shows well-defined lucent lesion without sclerotic rim. (Adapted and reprinted, with permission, from reference 1.) **(b)** Anteroposterior radiograph of femur shows well-defined geographic lytic focus of myeloma without a sclerotic rim. Notice the endosteal scalloping (arrows).

is usually located centrally within the medullary cavity, while an aneurysmal bone cyst is located eccentrically in the medullary cavity (Fig 1) (Table 2). However, in short or thin tubular bones, such as the metacarpals, metatarsals, phalanges, and fibula, the entire diameter of the bone can be involved, sometimes making it difficult to determine in what part of the bone the lesion started.

An apophysis (a growth center that does not contribute to the length of a bone) is the equivalent of an epiphysis (a growth center at the end of a bone that does contribute to length); thus, one should use the "end-of-bone" differential list for a lesion in such sites as the greater trochanter of the femur and the tibial tubercle (Fig 2). Similarly, other growth centers such as the patella; the small bones of the wrist, hindfoot, and midfoot; and the subarticular portions of flat bones, such as those around the sacroiliac joints and acetabuli in the pelvis and the glenoid of the scapula, are also end-of-bone equivalents (10).

The differential diagnosis can then be further narrowed by knowing the age of the patient. For example, a lytic lesion in the epiphysis of a long bone of an adolescent is likely to be a chondroblastoma, whereas a lytic lesion at the end of a long bone in a young adult is likely to be a giant cell tumor. Ewing sarcoma and Langerhans cell histiocytosis have a predilection for the diaphysis of long bones in people younger than 20 years and a predilection for flat bones such as the pelvis and skull in people older than 20 years (4), reflecting the normal change in the distribution of red marrow as a person ages.

Some processes have a predilection for a particular bone and location, such as an adamantinoma and osteofibrous dysplasia for the anterior cortex of the tibia (11), periosteal desmoid for the posterior distal aspect of the femur, and hemangioma for vertebral bodies (Table 3).

Table 3

Specific Sites of Selected Tumors

Tumor	Site
Adamantinoma	Anterior cortex of tibia
Osteofibrous dysplasia	Anterior cortex of tibia
Epidermal inclusion cyst	Terminal tuft of phalanx
Glomus tumor	Terminal tuft of phalanx
Periosteal desmoid	Posterior cortex of distal femur
Parosteal osteosarcoma	Posterior cortex of distal femur
Chordoma	Clivus, vertebral bodies, sacrum
Hemangioma	Vertebral bodies
Simple bone cyst	Calcaneus
Intraosseous lipoma	Calcaneus (may have focal calcification)
Osteoblastoma	Posterior elements of spine
Aneursymal bone cyst	Posterior elements of spine

Figure 5

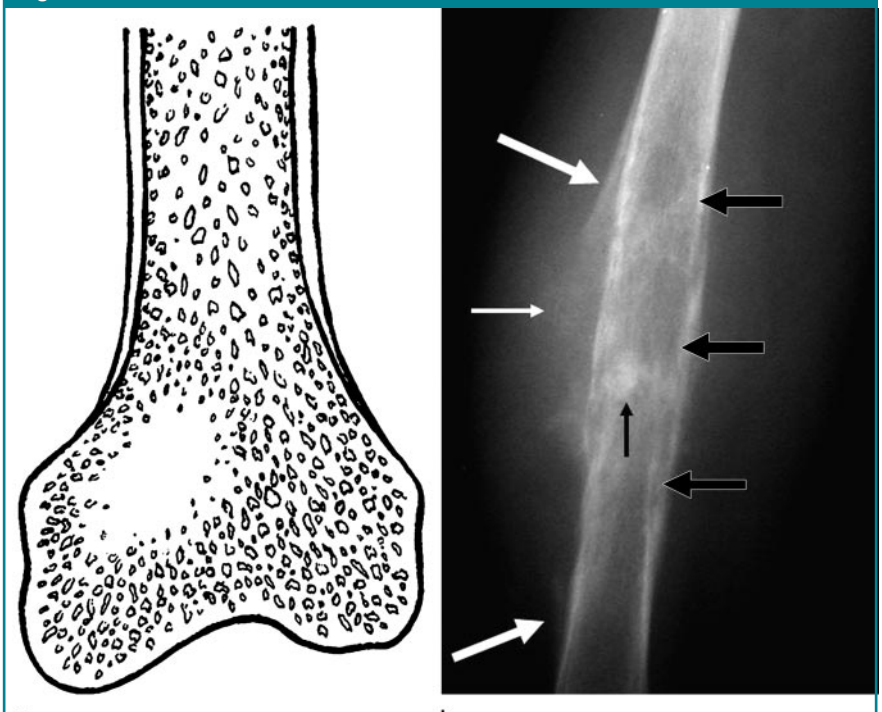

Figure 5: Type 1c geographic lesion. **(a)** Diagram shows ill-defined lytic lesion. (Adapted and reprinted, with permission, from reference 1.) **(b)** Lateral radiograph of femur in patient with osteosarcoma shows large ill-defined lytic lesion (large black arrows). Note Codman triangles (large white arrows), periosteal interruption (small white arrow), and tumor-induced new bone production (small black arrow). The diaphyseal location is unusual for osteosarcoma.

Margin

Bone lesions may range from a discrete well-defined abnormality to an ill-defined infiltrative process. The margin of the lesion and the zone of transition between lesion and adjacent bone are key factors in determining if a lesion is aggressive. A lesion with sharp margins and a narrow transition zone is radiographically considered nonaggressive, particularly when the margins have a sclerotic border.

A focal discrete lesion is called "geographic." Geographic lesions are classi-

Table 4

Tumors with a Permeated or Moth-eaten Appearance, by Age

Tumor Type	Patient Age
Benign	
Localized Langerhans cell histiocytosis	5–15 yr
Acute pyogenic osteomyelitis	Any age
Malignant	
Neuroblastoma metastases	Young child
Retinoblastoma metastases	Young child
Rhabdomyosarcoma metastases	Young child
Leukemia	Young child
Ewing sarcoma and variants (primitive neuroectodermal tumor, Askin tumor)	5–20 yr
Osteosarcoma	10–25 yr
Lymphoma	>20 yr
Myeloma	>40 yr

Table 5

Lesions That May Contain a Sequestrum

Lesion Character	Lesion
Benign	Chronic osteomyelitis
	Localized Langerhans cell histiocytosis
	Osteochondral fracture (osseous fragment in donor pit)
	Intraosseous lipoma (ossification of fat necrosis rather than true sequestrum)
Malignant	Fibrosarcoma
	Malignant fibrous histiocytoma
	Primary lymphoma of bone

Table 6

Multiple Bone Lesions

Lesion Characteristic	Lesion
Sclerotic	Multiple bone islands (osteopoikilosis)
	Osteoblastic metastatic carcinoma (prostate, breast, lung, colon, mucin-producing adenocarcinoma)
Lytic	Osteolytic metastatic carcinoma (prostate, breast, lung, colon, etc)
	Myeloma
	Non-Hodgkin lymphoma
	Benign vascular lesions: hemangioma, cystic angiomatosis (rare tumor)
	Malignant vascular lesions (rare tumors): hemangioendothelioma, angiosarcoma, hemangiopericytoma
	Brown tumors of hyperparathyroidism (should have other radiographic features of hyperparathyroidism)
	Multiple enchondromatosis (Ollier and Maffuci disease; may have internal mineralization or appear as lucent linear seams of cartilage within bone)
	Fibrous dysplasia (usually ground-glass lytic but may be mixed lytic and sclerotic; bone may be deformed)

fied as type 1 and can be further categorized as type 1a (well-defined border with sclerotic rim) (Fig 3), type 1b (well-defined border but without sclerotic rim) (Fig 4), and type 1c (focal lytic lesion with ill-defined border) (Fig 5) (1). On the other hand, an infiltrative lesion has ill-defined margins and a broad zone of transition, and its pattern of bone destruction may be "moth-eaten" (type 2) (Fig 6) or "permeated" (type 3) (Fig 7), which refer to small, patchy, ill-defined areas of lytic bone destruction.

The classification of a lesion is not as important as an understanding of the radiographic features that make the abnormality look innocuous or aggressive. Type 1a lesions are at one end of the spectrum as the most innocuous and nonaggressive appearing, and type 3 lesions are at the other end of the spectrum as the most aggressive appearing. However, while a nonaggressive appearance suggests a benign process and an aggressive appearance suggests a malignant one, this is not always the case: Osteomyelitis and localized Langerhans cell histiocytosis are benign processes that can have an aggressive permeated appearance, and a giant cell tumor may look well defined but be locally aggressive and, on rare occasions, may even metastasize.

The permeated appearance is typical of a class of malignant lesions called the "small round blue cell group" because of these lesions' histologic appearance on hematoxylin and eosin stained specimens (12–14). Osteomyelitis and localized Langerhans cell histiocytosis also look "blue" on hematoxylin and eosin stained specimens. Although they are not histologically the same as the malignant small round blue cell lesions, they may also cause a permeated or moth-eaten radiographic appearance (Table 4).

Periosteal Reaction

The presence and appearance of periosteal reaction are also important radiographic features that help characterize a bone lesion. Solid or unilamellated periosteal reaction is a nonaggressive ap-

pearance, since it indicates that the underlying lesion is slow growing and is giving the bone a chance to wall the lesion off (Fig 8). A multilamellated or "onionskin" appearance suggests an intermediate aggressive process, such as one that waxes and wanes or one that the bone is continually trying to wall off but cannot (4) (Figs 6, 9). Interruption (ie, regional disruption) of either the uni- or multilamellated periosteal reaction suggests an aggressive process that has broken through the periosteum. A spiculated, or "hair-on-end" (perpendicular to the cortex) or sunburst pattern, is the most aggressive appearance and is highly suggestive of malignancy (Fig 10). A Codman triangle refers to elevation of the periosteum away from the cortex, with an angle formed where the elevated periosteum and bone come together (Figs 5, 11); although the Codman triangle is often associated with conventional osteosarcoma, any aggressive process that lifts the periosteum may produce this appearance, even benign entities such as infection and subperiosteal hematoma. Sometimes periosteal reaction occurs as a result of pathologic fracture through a bone tumor and not because of the tumor itself, such as in the case of a simple bone cyst.

Opacity and Mineralization

Tumors may be lytic, sclerotic, or mixed and usually have a typical opacity. For example, simple bone cysts and giant cell tumors are lytic, bone islands are sclerotic, and adamantinomas are often mixed. Lucency and sclerosis associated with true neoplasms are due to stimulation of osteoclasts or osteoblasts, respectively, by the tumor. Sometimes the destructive process will cause a fragment of bone to become sequestered within the lytic region; such a sequestrum may be seen in both benign and malignant processes (15) (Table 5).

Occasionally, the trabecular pattern within the lesion is the clue to its diagnosis. For example, an aneurysmal bone cyst and a desmoplastic fibroma may have a honeycomb appearance (Fig 12), and Paget disease can have coarsened trabeculae. A hemangioma in a long bone may have a sunburst or spoke-and-wheel pattern of trabeculation, while this same entity in a vertebral body will have a vertically oriented, coarsened, "corduroy" trabecular pattern.

The radiographic opacity of a lesion can also be affected by the mineralization of its matrix. The term *matrix* refers to the type of tissue of the tumor—such as osteoid, chondral, fibrous, or adipose, all of which are radiolucent—and *mineralization* refers to calcification of the matrix. This concept of matrix mineralization is important to understand, because the pattern of mineralization can be a clue

Figure 6

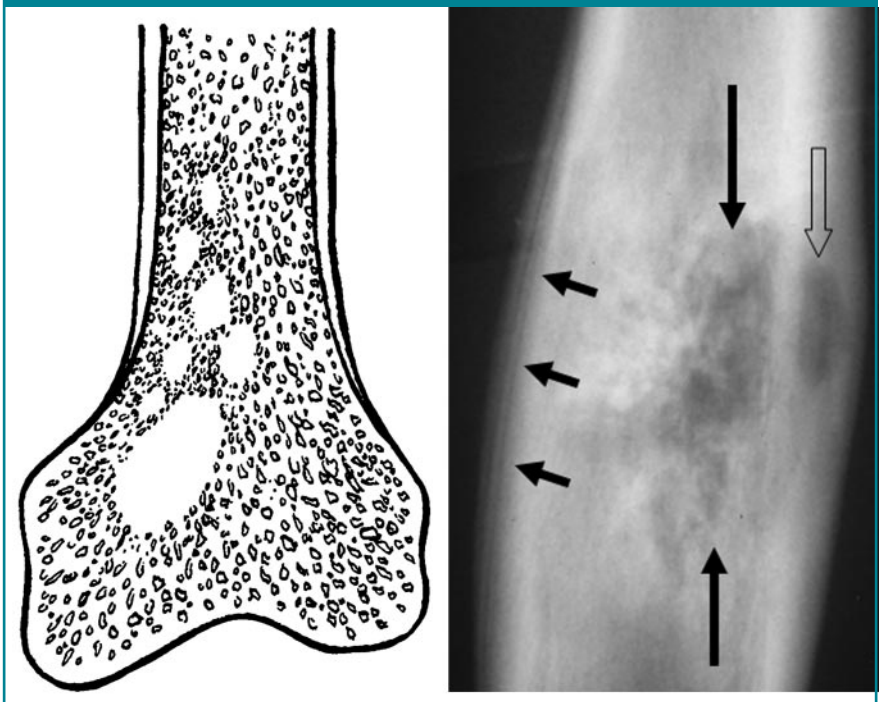

Figure 6: Type 2 moth-eaten lesion. **(a)** Diagram shows patchy lysis of medullary cavity. (Adapted and reprinted, with permission, from reference 1.) **(b)** Anteroposterior radiograph of osteosarcoma shows ill-defined patchy lytic lesion involving medullary cavity (long solid arrows) and cortex (open arrow). Also note multilamellated periosteal reaction (short solid arrows).

Table 7

Lytic Expansile Soap Bubble Appearance

Lesion Character	Lesion
Benign	Aneurysmal bone cyst
	Nonossifying fibroma
	Chondromyxoid fibroma
	Brown tumor of hyperparathyroidism (should have other radiographic features of hyperparathyroidism)
	Hemophiliac pseudotumor (should also have hemophiliac arthropathy)
Malignant	Metastasis (especially renal and thyroid carcinoma)
	Plasmacytoma
	Telangiectatic osteosarcoma

Figure 7

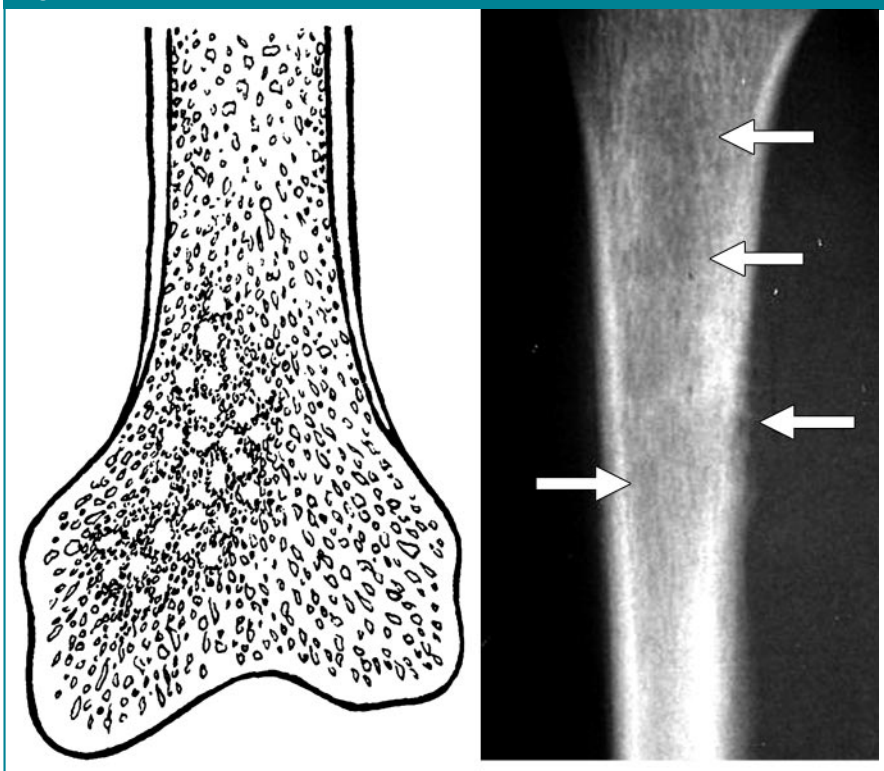

Figure 7: Type 3 permeated lytic lesion. **(a)** Diagram shows small patchy lucencies in medullary cavity. (Adapted and reprinted, with permission, from reference 1.) **(b)** Anteroposterior radiograph shows fine permeated pattern involving cortex and medullary space of diametaphysis of proximal portion of tibia (arrows) in a patient with Ewing sarcoma. (Image courtesy of Marcia Blacksin, MD, University of Medicine and Dentistry of New Jersey, Newark, NJ.)

Figure 8

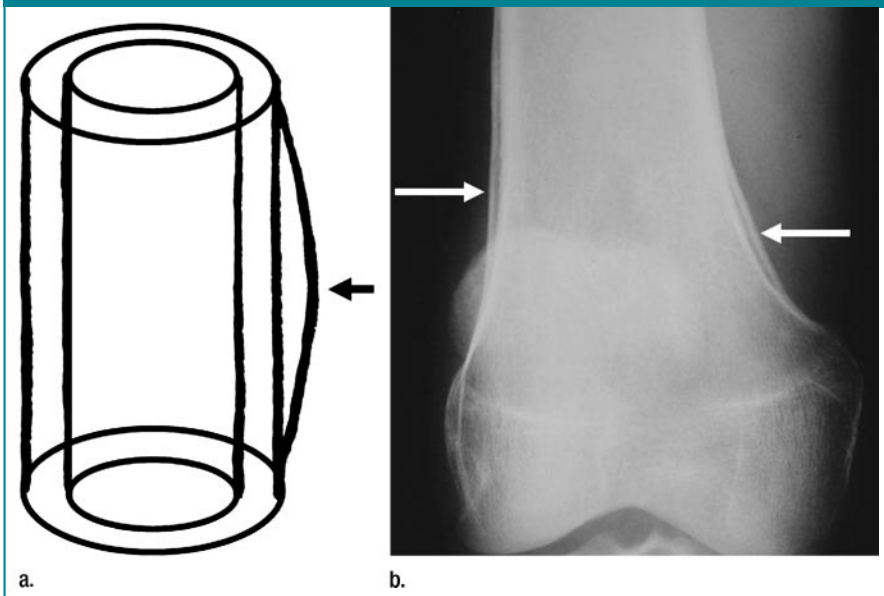

Figure 8: Unilamellated periosteal reaction. **(a)** Diagram shows single layer of reactive periosteum (arrow). (Adapted and reprinted, with permission, from reference 2.) **(b)** Anteroposterior radiograph of the knee in patient with hypertrophic osteoarthropathy shows thick unilamellated periosteal reaction (arrows).

Figure 9

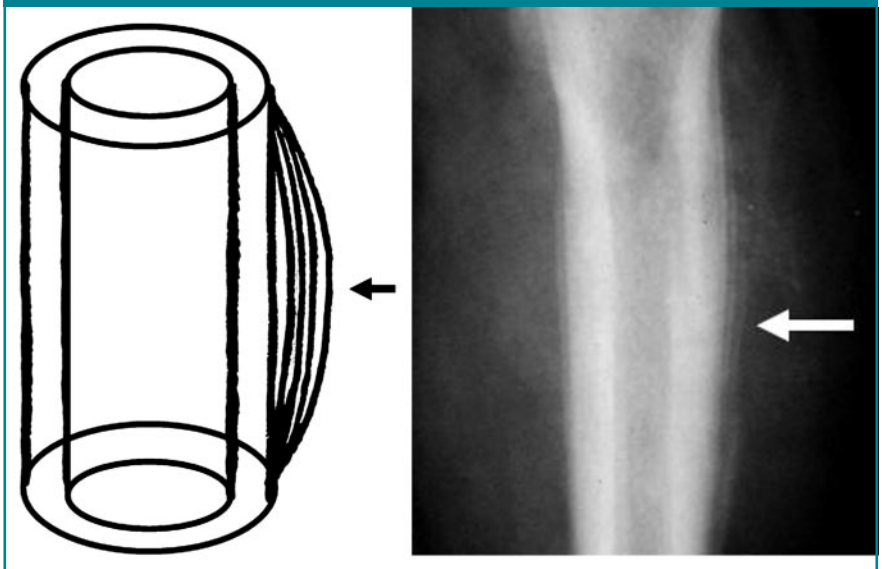

Figure 9: Multilamellated periosteal reaction. **(a)** Diagram shows multilamellated, or onionskin, periosteal reaction (arrow). (Adapted and reprinted, with permission, from reference 2.) **(b)** Anteroposterior radiograph in a patient with osteosarcoma shows multilamellated periosteal reaction (arrow) in proximal portion of femur. Note also large surrounding soft-tissue mass. See also Figure 6b. (Image courtesy of David Disler, MD, Commonwealth Radiology, Richmond, Va.)

Figure 11

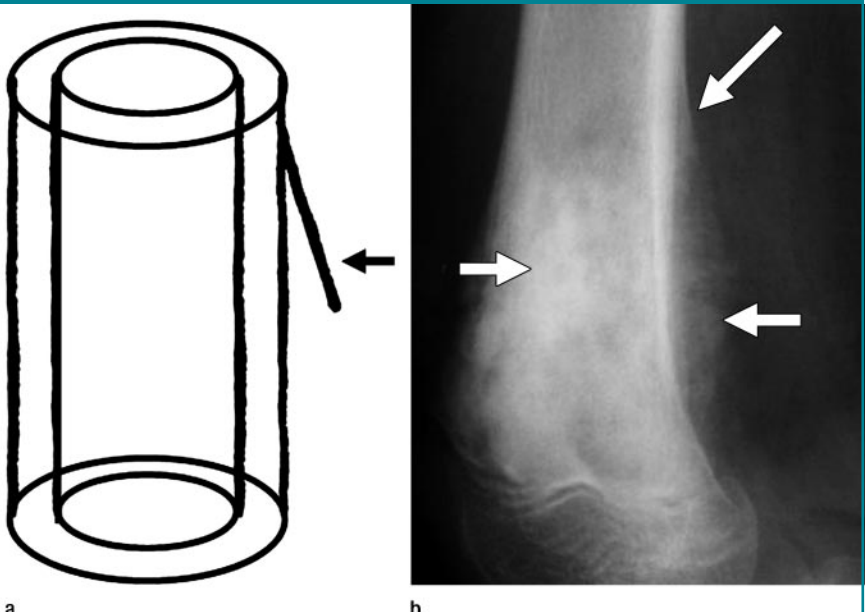

Figure 11: Codman triangle. **(a)** Diagram shows elevated periosteum (arrow) forming an angle with the cortex. (Adapted and reprinted, with permission, from reference 2.) **(b)** Lateral radiograph in patient with osteosarcoma shows the elevated periosteum forming Codman triangle (long arrow). Notice the tumor-induced new bone formation (short arrows.) See also Figure 5b.

to the type of underlying matrix and, thus, the diagnosis. For example, calcification of chondral tissue often produces punctate, flocculent, comma-shaped, or arclike or ringlike mineralization, indicating that the lesion is cartilaginous, such as an enchondroma, chondrosarcoma, or chondroblastoma (Fig 13), but all of these lesions vary in the frequency of radiographically evident mineralization. Bone-forming tumors have fluffy, amorphous, cloudlike mineralization, causing an opaque radiographic appearance (Figs 5, 11, 14), but the distinction between chondral and osseous mineralization can sometimes be difficult. Some tumors are completely nonmineralized, making determination of their tissue of origin difficult. Faint mineralization in a lesion is best assessed by using CT, which is more sensitive than radiographs for differences in attenuation (16–18).

Size and Number

The size of a lesion can also be a clue to its diagnosis, since some entities have size criteria. For example, osteoid osteoma and osteoblastoma are histologically similar lesions, but they differ in size: The nidus of an osteoid osteoma is less than 1.5 cm in diameter, while the osteoblastoma is larger than 1.5 cm (19). Traditionally, a well-defined lytic lesion in the cortex of a long bone with a sclerotic rim has been termed a fibrous cortical defect if it is less than 3 cm in length and a nonossifying fibroma if it is larger than 3 cm (10), but some authors prefer to use the term fibroxanthoma for both of these lesions (20). A 1–2-cm chondral lesion in a long bone is most likely to be an enchondroma, while the risk of it being a low-grade chondrosarcoma increases if it is greater than 4 or 5 cm (21–24).

Primary bone tumors are solitary occurrences, while other abnormalities may be multiple (Table 6). Multiple sclerotic lesions might represent metastatic disease or osteopoikolosis (multiple bone islands); the latter are usually similar in size and are centered around joints. The most common causes of multiple lucencies in someone older

Figure 10

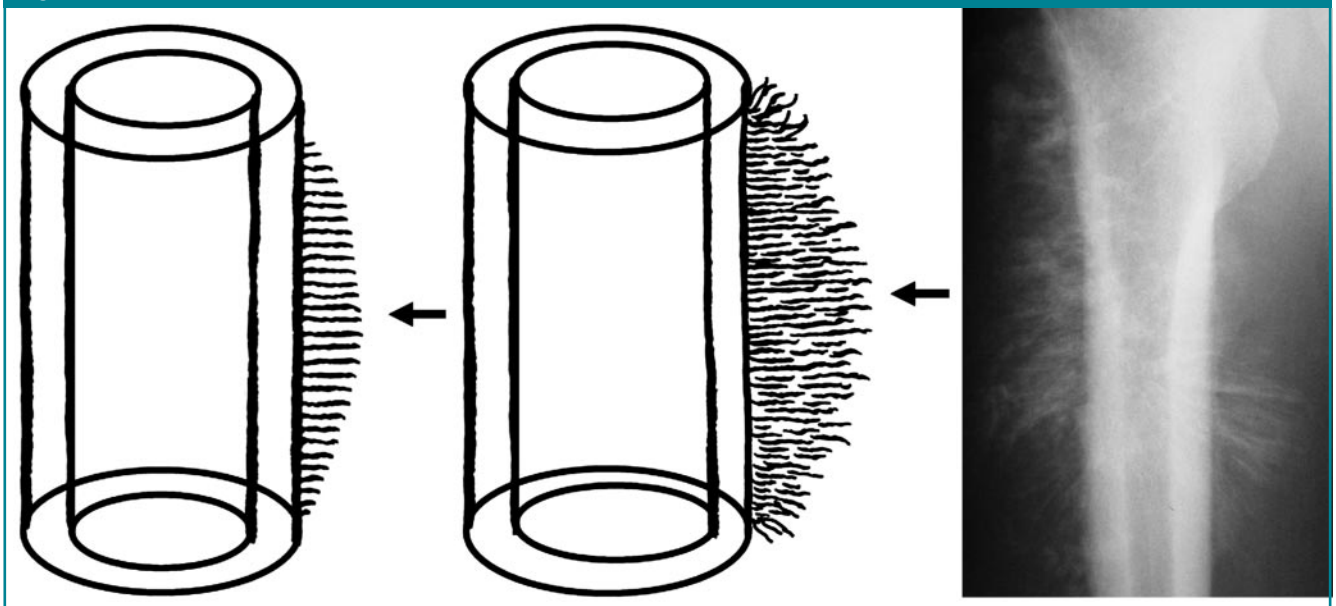

Figure 10: Perpendicular periosteal reaction. **(a)** Diagram shows spiculated, or hair-on-end, periosteal reaction (arrow). **(b)** Diagram shows radial, or sunburst, periosteal reaction (arrow). (Fig 10a, 10b adapted and reprinted, with permission, from reference 2.) **(c)** Anteroposterior radiograph in patient with osteosarcoma shows marked perpendicular periosteal reaction in proximal portion of femur. (Image courtesy of Marcia Blacksin, MD, University of Medicine and Dentistry of New Jersey, Newark, NJ.)

Figure 12

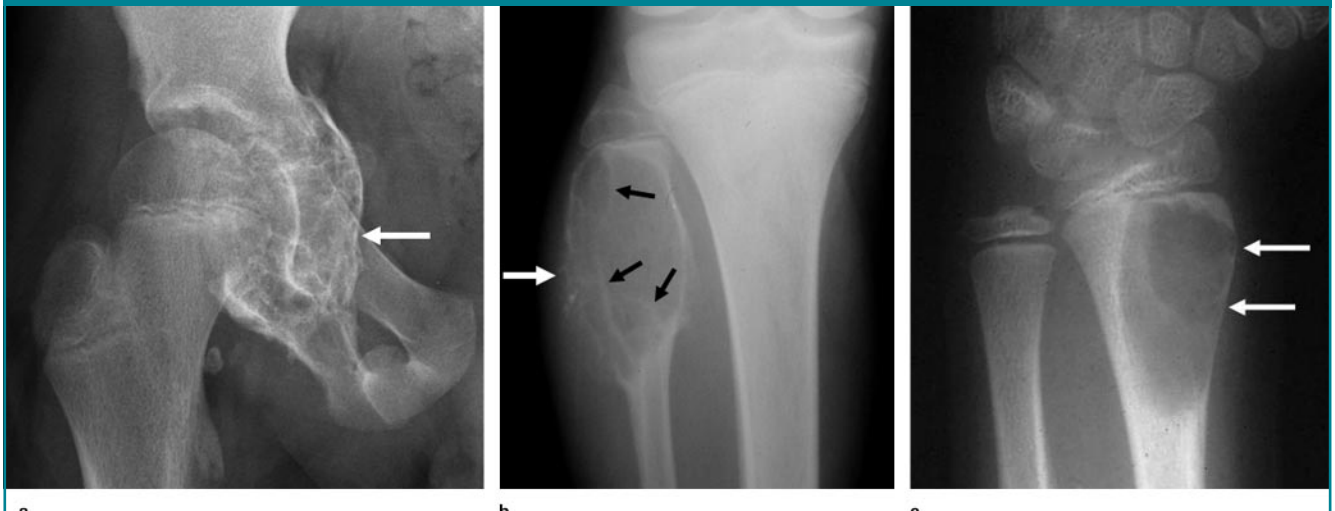

Figure 12: Aneurysmal bone cysts. **(a)** Anteroposterior radiograph of the pelvis shows expansile lytic lesion of right acetabulum with thinning of the cortex (arrow) and honeycomb trabeculation. Flat bones are a common location for aneurysmal bone cysts. (Image courtesy of Marcia Blacksin, MD, University of Medicine and Dentistry of New Jersey, Newark, NJ.) **(b)** Anteroposterior radiograph of proximal portion of tibia and fibula shows expansile lytic lesion in proximal fibular metaphysis, with mild honeycombing (black arrows). Eccentric origin of the lesion is hard to appreciate in thin bones such as the fibula; both cortices are ballooned, with focal loss laterally (white arrow). (Image courtesy of David Disler, MD, Commonwealth Radiology, Richmond, Va.) **(c)** Anteroposterior radiograph of distal forearm and wrist shows more typical eccentric location of aneurysmal bone cyst in distal metaphysis of the radius, although this particular lesion lacks a honeycomb appearance. Cortex on radial side is very thin (arrows). (Image courtesy of Bernard Ghelman, MD, Hospital for Special Surgery, New York, NY.)

than 40 years are metastatic carcinoma, multiple myeloma, and metastatic non-Hodgkin lymphoma, but benign entities such as multiple brown tumors may look similar.

Cortical Involvement

In addition to lesions that specifically arise within the cortex, the cortex may be affected by processes that originate in the medullary canal or the periosteum or surrounding soft tissue. For example, as a medullary process expands, it may cause erosion of the inner surface of the cortex, called *endosteal scalloping* (Fig 4). If the medullary lesion is so aggressive that it erodes the inner aspect of the cortex without giving the periosteum a chance to lay down new bone, the cortex will eventually be completely destroyed and breached by the lesion. On the other hand, if the bone has time to lay down new periosteum on the outer surface of the cortex as the inner surface is being eroded, the bone may look expanded owing to the outward ballooning of the cortex (Fig 12). Depending on the aggressiveness of the lesion, the ballooned cortex may have normal thickness or be thin. The ballooned cortex gives rise to the catego-

Figure 13

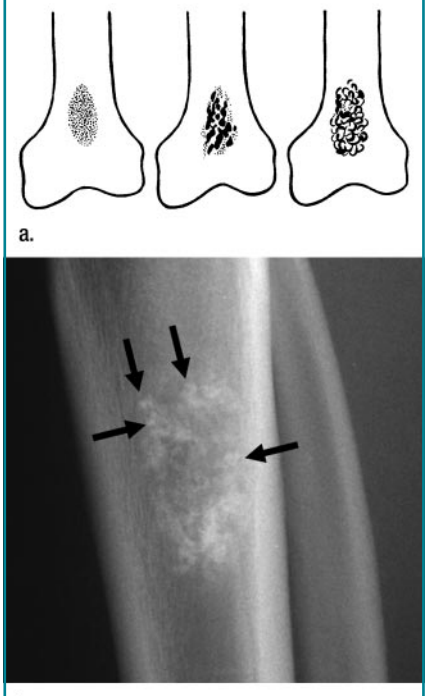

Figure 13: Chondral mineralization. **(a)** Diagram shows patterns and of mineralization of cartilaginous tumor matrix: stippled (left), flocculent (middle), and ring and arc (right). (Adapted and reprinted, with permission, from reference 3.) **(b)** Lateral radiograph of proximal portion of tibia shows enchondroma with punctate and arclike mineralization (arrows).

Figure 14

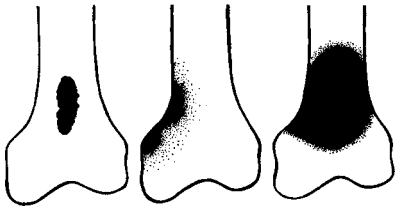

Figure 14: Diagram shows patterns of mineralization of osseous matrix with solid (left), cloud-like (middle), and ivory-like (right) opacity. (Adapted and reprinted, with permission, from reference 3.) See also Figures 5b, 11b, and 16.

Figure 16

Figure 16: Lateral radiograph of distal portion of femur shows osteosarcoma with amorphous tumor-induced new bone formation (black arrows). Note the large soft-tissue mass (white arrows) that displaces adjacent fat.

Figure 15

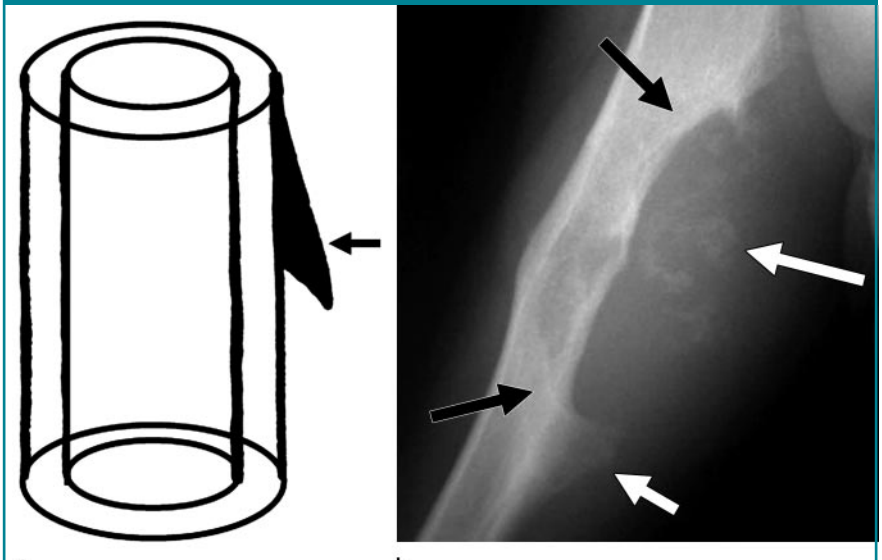

Figure 15: Buttress periosteal reaction. **(a)** Diagram shows beaklike solid periosteal buttress formation (arrow). (Adapted and reprinted, with permission, from reference 2.) **(b)** Anteroposterior radiograph of humerus in a patient with periosteal chondrosarcoma shows periosteal buttress (short white arrow). Note well-defined saucerization of humeral shaft (black arrows) and faint mineralization of the matrix (long white arrow).

ries of lytic expansile and "soap bubble" lesions (Table 7).

A process that starts on the outer surface of the cortex, either in the periosteum or adjacent soft tissue, may erode the outer surface of the cortex; this process is called *saucerization*. If the tumor is not mineralized, saucerization may be the only radiographic indication of its presence. Sometimes the periosteum will react at the site adjacent to the saucerization, giving a buttressed appearance but not necessarily indicating the benign or malignant nature of the lesion (Fig 15). The buttressed appearance may also occur when a slowly growing intramedullary process becomes more aggressive and breaks through (ie, interrupts) an area of solid periosteal reaction.

Soft-Tissue Component

The presence of a soft-tissue component with a bone lesion suggests a malignant process. The tumor may have frankly destroyed the cortex as it expanded, or it may have permeated through the haversian canals of the cortex to reach the surrounding tissue. The soft-tissue component may displace adjacent fat planes (Fig 16). Tumors that often have a soft-tissue component are osteosarcoma, Ewing sarcoma, and lymphoma (25–27).

Advanced Imaging

While radiographs are often sufficient to enable a diagnosis, advanced imaging is sometimes needed. MR images and CT scans may provide additional information by virtue of their tomographic nature, multiplanar capability, and better soft-tissue contrast than radiographs. CT is useful for evaluating subtle mineralization in a lytic lesion, for demonstrating radiographically occult bone destruction (16–18), or for demonstrating the lucent nidus of an osteoid osteoma amid a large area of reactive sclerosis (28). MR imaging has become the standard for evaluating the local extent of a malignant process for the purposes of staging (29,30) and assessing tumor response to chemotherapy (31–33). However, it must be stressed that CT and MR images should only be interpreted with concurrent radiographic correlation.

Conclusion

Despite the availability of advanced imaging methods such as CT and MR imaging, with their ever increasing number of detectors and strength of the magnetic field, the diagnosis of a tumor or tumorlike lesion of bone still depends on the conventional radiograph. By paying attention to the age of the patient, the location of the lesion, and the radiographic features of the lesion, the interpreter will be led to a short differential, if not the single correct, diagnosis.

Acknowledgment: I thank Robert Villani, MD, one of my former residents, for his excellent adaptations of the original drawings.

References

1. Madewell JE, Ragsdale BD, Sweet DE. Radiologic and pathologic analysis of solitary bone lesions. I. Internal margins. Radiol Clin North Am 1981;19:715–748.
2. Ragsdale BD, Madewell JE, Sweet DE. Radiologic and pathologic analysis of solitary bone lesions. II. Periosteal reactions. Radiol Clin North Am 1981;19:749–783.
3. Sweet DE, Madewell JE, Ragsdale BD. Radiologic and pathologic analysis of solitary bone lesions. III. Matrix patterns. Radiol Clin North Am 1981;19:785–814.
4. Kricun ME. Radiographic evaluation of solitary bone lesions. Orthop Clin North Am 1983;14:39–64.
5. Priolo F, Cerase A. The current role of radiography in the assessment of skeletal tumors and tumor-like lesions. Eur J Radiol 1998; 27(suppl 1):S77–S85.
6. Brown KT, Kattapuram SV, Rosenthal DI. Computed tomography analysis of bone tumors: patters of cortical destruction and soft tissue extension. Skeletal Radiol 1986; 15:448–451.
7. Seeger LL, Dungan DH, Eckardt JJ, Bassett LW, Gold RH. Nonspecific findings on MR imaging: the importance of correlative studies and clinical information. Clin Orthop Relat Res 1991;270:306–312.
8. Hayes CW, Conway WF, Sundaram M. Misleading aggressive MR imaging appearance of some benign musculoskeletal lesions. RadioGraphics 1992;12:1119–1136.
9. Ma LD, Frassica FJ, Scott WW, Fishman EK, Zerhouni EA. Differentiation of benign and malignant musculoskeletal tumors: potential pitfalls with MR imaging. RadioGraphics 1995;15:349–366.
10. Resnick D. Diagnosis of bone and joint disorders. 4th ed. Philadelphia, Pa: Saunders, 2002;3757:3922–3924.
11. Levine SM, Lambiase RE, Petchprapa CN. Cortical lesions of the tibia: characteristic appearances at conventional radiography. RadioGraphics 2003;23:157–177.
12. Roessner A, Jurgens H. Round cell tumours of bone. Pathol Res Pract 1993;189:111–136.
13. Pritchard DJ. Small round cell tumors. Orthop Clin North Am 1989;20:367–375.
14. Llombart-Bosch A, Contesso G, Peydro-Olaya A. Histology, immunohistochemistry, and electron microscopy of small round cell tumors of bone. Semin Diagn Pathol 1996; 13:153–170.
15. Mulligan ME, Kransdorf MJ. Sequestra in primary lymphoma of bone: prevalence and radiologic features. AJR Am J Roentgenol 1993;160:1245–1248.
16. Cerase A, Priolo F. Skeletal benign bone-forming lesions. Eur J Radiol 1998;27(suppl 1):S91–S97.
17. Pettersson H, Gillespy T 3rd, Hamlin DJ, et al. Primary musculoskeletal tumors: examination with MR imaging compared with conventional modalities. Radiology 1987; 164:237–241.
18. Zimmer WD, Berquist TH, McLeod RA, et al. Bone tumors: magnetic resonance imaging versus computed tomography. Radiology 1985;155:709–718.
19. White LM, Kandel R. Osteoid-producing tumors of bone. Semin Musculoskelet Radiol 2000;4:25–43.
20. Smith SE, Kransdorf MJ. Primary musculoskeletal tumors of fibrous origin. Semin Musculoskelet Radiol 2000;4:73–88.
21. Kendell SD, Collins MS, Adkins MC, Sundaram M, Unni KK. Radiographic differentiation of enchondroma from low-grade chondrosarcoma in the fibula. Skeletal Radiol 2004;33:458–466.
22. Geirnaerdt MJ, Hermans J, Bloem JL, et al. Usefulness of radiography in differentiating enchondroma from central grade 1 chondrosarcoma. AJR Am J Roentgenol 1997;169: 1097–1104.
23. Flemming DJ, Murphey MD. Enchondroma and chondrosarcoma. Semin Musculoskelet Radiol 2000;4:59–71.

24. Murphey MD, Flemming DJ, Boyea SR, Bojescul JA, Sweet DE, Temple HT. Enchondroma versus chondrosarcoma in the appendicular skeleton: differentiating features. RadioGraphics 1998;18:1213–1237.

25. Murphey MD, Robbin MR, McRae GA, Flemming DJ, Temple HT, Kransdorf MJ. The many faces of osteosarcoma. RadioGraphics 1997;17:1205–1231.

26. Kransdorf MJ, Smith SE. Lesions of unknown histogenesis: Langerhans cell histiocytosis and Ewing sarcoma. Semin Musculoskelet Radiol 2000;4:113–125.

27. Mulligan ME. Myeloma and lymphoma. Semin Musculoskelet Radiol 2000;4:127–135.

28. Assoun J, Richardi G, Railhac JJ, et al. Osteoid osteoma: MR imaging versus CT. Radiology 1994;191:217–223.

29. Norton KI, Hermann G, Abdelwahab IF, Klein MJ, Granowetter LF, Rabinowitz JG. Epiphyseal involvement in osteosarcoma. Radiology 1991;180:813–816.

30. Panicek DM, Gatsonis C, Rosenthal DI, et al. CT and MR imaging in the local staging of primary malignant musculoskeletal neoplasms: report of the Radiology Diagnostic Oncology Group. Radiology 1997;202:237–246.

31. Lang P, Grampp S, Vahlensieck M, et al. Primary bone tumors: value of MR angiography for preoperative planning and monitoring response to chemotherapy. AJR Am J Roentgenol 1995;165:135–142.

32. van der Woude HJ, Bloem JL, Verstraete KL, Taminiau AH, Nooy MA, Hogendoorn PC. Osteosarcoma and Ewing's sarcoma after neoadjuvant chemotherapy: value of dynamic MR imaging in detecting viable tumor before surgery. AJR Am J Roentgenol 1995; 165:593–598.

33. van der Woude HJ, Bloem JL, Hogendoorn PC. Preoperative evaluation and monitoring chemotherapy in patients with high-grade osteogenic and Ewing's sarcoma: review of current imaging modalities. Skeletal Radiol 1998;27:57–71.

Radiology 2008

This is your reprint order form or pro forma invoice

(Please keep a copy of this document for your records.)

Reprint order forms and purchase orders or prepayments must be received 72 hours after receipt of form either by mail or by fax at 410-820-9765. It is the policy of Cadmus Reprints to issue one invoice per order. **Please print clearly**.

Author Name _____
Title of Article _____
Issue of Journal_____ Reprint # _____ Publication Date _____
Number of Pages_____ KB # _____ Symbol Radiology
Color in Article? Yes / No (Please Circle)

Please include the journal name and reprint number or manuscript number on your purchase order or other correspondence.

Order and Shipping Information

Reprint Costs **(Please see page 2 of 2 for reprint costs/fees.)**

_____ Number of reprints ordered $_____
_____ Number of color reprints ordered $_____
_____ Number of covers ordered $_____
Subtotal $_____
Taxes $_____

(*Add appropriate sales tax for Virginia, Maryland, Pennsylvania, and the District of Columbia or Canadian GST to the reprints if your order is to be shipped to these locations*.)

First address included, add $32 for each additional shipping address $_____

TOTAL $_____

Shipping Address **(cannot ship to a P.O. Box) Please Print Clearly**

Name _____
Institution _____
Street _____
City _____ State _____ Zip _____
Country _____
Quantity_____ Fax _____
Phone: Day _____ Evening _____
E-mail Address _____

Additional Shipping Address* **(cannot ship to a P.O. Box)**

Name _____
Institution _____
Street _____
City _____ State _____ Zip _____
Country _____
Quantity _____ Fax _____
Phone: Day _____ Evening _____
E-mail Address _____
** Add $32 for each additional shipping address*

Payment and Credit Card Details

Enclosed: Personal Check _____
Credit Card Payment Details _____
Checks must be paid in U.S. dollars and drawn on a U.S. Bank.

Credit Card: __ VISA __ Am. Exp. __ MasterCard
Card Number _____
Expiration Date_____
Signature: _____

Please send your order form and prepayment made payable to:

Cadmus Reprints
P.O. Box 751903
Charlotte, NC 28275-1903

Note: Do not send express packages to this location, PO Box.
FEIN #:541274108

Invoice or Credit Card Information

Invoice Address Please Print Clearly
Please complete Invoice address as it appears on credit card statement

Name _____
Institution _____
Department _____
Street _____
City _____ State _____ Zip _____
Country _____
Phone _____ Fax _____
E-mail Address _____

Cadmus will process credit cards and *Cadmus Journal Services* will appear on the credit card statement.

If you don't mail your order form, you may fax it to 410-820-9765 with your credit card information.

Signature _____ Date _____
Signature is required. By signing this form, the author agrees to accept the responsibility for the payment of reprints and/or all charges described in this document.

RB-9/26/07

Radiology 2008

Black and White Reprint Prices

Domestic (USA only)						
# of Pages	50	100	200	300	400	500
1-4	$221	$233	$268	$285	$303	$323
5-8	$355	$382	$432	$466	$510	$544
9-12	$466	$513	$595	$652	$714	$775
13-16	$576	$640	$749	$830	$912	$995
17-20	$694	$775	$906	$1,017	$1,117	$1,220
21-24	$809	$906	$1,071	$1,200	$1,321	$1,471
25-28	$928	$1,041	$1,242	$1,390	$1,544	$1,688
29-32	$1,042	$1,178	$1,403	$1,568	$1,751	$1,924
Covers	$97	$118	$215	$323	$442	$555

International (includes Canada and Mexico)						
# of Pages	50	100	200	300	400	500
1-4	$272	$283	$340	$397	$446	$506
5-8	$428	$455	$576	$675	$784	$884
9-12	$580	$626	$805	$964	$1,115	$1,278
13-16	$724	$786	$1,023	$1,232	$1,445	$1,652
17-20	$878	$958	$1,246	$1,520	$1,774	$2,030
21-24	$1,022	$1,119	$1,474	$1,795	$2,108	$2,426
25-28	$1,176	$1,291	$1,700	$2,070	$2,450	$2,813
29-32	$1,316	$1,452	$1,936	$2,355	$2,784	$3,209
Covers	$156	$176	$335	$525	$716	$905

Color Reprint Prices

Domestic (USA only)						
# of Pages	50	100	200	300	400	500
1-4	$223	$239	$352	$473	$597	$719
5-8	$349	$401	$601	$849	$1,099	$1,349
9-12	$486	$517	$852	$1,232	$1,609	$1,992
13-16	$615	$651	$1,105	$1,609	$2,117	$2,624
17-20	$759	$787	$1,357	$1,997	$2,626	$3,260
21-24	$897	$924	$1,611	$2,376	$3,135	$3,905
25-28	$1,033	$1,071	$1,873	$2,757	$3,650	$4,536
29-32	$1,175	$1,208	$2,122	$3,138	$4,162	$5,180
Covers	$97	$118	$215	$323	$442	$555

International (includes Canada and Mexico))						
# of Pages	50	100	200	300	400	500
1-4	$278	$290	$424	$586	$741	$904
5-8	$429	$472	$746	$1,058	$1,374	$1,690
9-12	$604	$629	$1,061	$1,545	$2,011	$2,494
13-16	$766	$797	$1,378	$2,013	$2,647	$3,280
17-20	$945	$972	$1,698	$2,499	$3,282	$4,069
21-24	$1,110	$1,139	$2,015	$2,970	$3,921	$4,873
25-28	$1,290	$1,321	$2,333	$3,437	$4,556	$5,661
29-32	$1,455	$1,482	$2,652	$3,924	$5,193	$6,462
Covers	$156	$176	$335	$525	$716	$905

Minimum order is 50 copies. For orders larger than 500 copies, please consult Cadmus Reprints at 800-407-9190.

Reprint Cover

Cover prices are listed above. The cover will include the publication title, article title, and author name in black.

Shipping

Shipping costs are included in the reprint prices. Domestic orders are shipped via UPS Ground service. Foreign orders are shipped via a proof of delivery air service.

Multiple Shipments

Orders can be shipped to more than one location. Please be aware that it will cost $32 for each additional location.

Delivery

Your order will be shipped within 2 weeks of the journal print date. Allow extra time for delivery.

Tax Due

Residents of Virginia, Maryland, Pennsylvania, and the District of Columbia are required to add the appropriate sales tax to each reprint order. For orders shipped to Canada, please add 7% Canadian GST unless exemption is claimed.

Ordering

Reprint order forms and purchase order or prepayment is required to process your order. Please reference journal name and reprint number or manuscript number on any correspondence. You may use the reverse side of this form as a proforma invoice. Please return your order form and prepayment to:

Cadmus Reprints
P.O. Box 751903
Charlotte, NC 28275-1903

Note: Do not send express packages to this location, PO Box.
FEIN #:541274108

Please direct all inquiries to:

Rose A. Baynard
800-407-9190 (toll free number)
410-819-3966 (direct number)
410-820-9765 (FAX number)
baynardr@cadmus.com (e-mail)

Reprint Order Forms and purchase order or prepayments must be received 72 hours after receipt of form.